Regular Article

Microstructure and thermal properties of RETaO$_4$ (RE = Nd, Eu, Gd, Dy, Er, Yb, Lu) as promising thermal barrier coating materials

Jun Wang, XiaoYu Chong, Rong Zhou, Jing Feng *

Faculty of Material Science and Engineering, Kunming University of Science and Technology, Kunming 650093, People's Republic of China

A B S T R A C T

The RETaO$_4$ ceramics with low-thermal conductivity were fabricated using a solid-state reaction. The phase composition and microstructures of high-temperature RETaO$_4$ (RE = Nd, Eu, Gd, Dy, Er, Yb, Lu) ceramics were characterized by X-ray diffraction (XRD), scanning electron microscope (SEM) and Raman spectroscopy. The RETaO$_4$ ceramics had lower thermal conductivity (1.38 to 1.94 W·m^{-1}·K^{-1} at 800 °C) than 7-8YSZ (2.37 and 2.47 W·m^{-1}·K^{-1} at 800 °C, respectively). The porosity significantly affected the thermal conductivity of RETaO$_4$ ceramics. The RETaO$_4$ ceramics also had lower Vickers hardness than 8YSZ, which suggests that RETaO$_4$ has better fracture toughness and thermal tolerance.

© 2016 Acta Materialia Inc. Published by Elsevier Ltd. All rights reserved.

Ceramic thermal barrier coatings (TBCs) are used in gas turbines to protect the metal parts from hot burner gases. TBCs can decrease the operation temperature between the gas turbine and the surface of its parts [1,2]. Yttria-stabilized zirconia (7-8YSZ) has relatively low thermal conductivity (2–3 W.m^{-1} k^{-1}), a high coefficient of thermal expansion (approximately 10×10^{-6} K^{-1}) and excellent mechanical properties [3–5]. However, 7-8YSZ has problems when the temperature exceeds 1200 °C because of its phase transformation: the t' phase may decompose into cubic (c) and tetragonal (t) phases during the high-temperature operation, and the latter is susceptible to the disruptive martensitic transformation to the monoclinic phase (m), which severely destroys the coatings [6–7]. The phase transformation and deterioration of mechanical properties cause high thermal stresses and consequently a lifetime reduction. To increase the operated temperature of TBCs, new materials of TBCs are urgently required. YTaO$_4$, one type of TBC, was expected to exceed 1600 °C in our previous study [8]. Moreover, we plan to use RETaO$_4$ (RE = Nd, Eu, Gd, Dy, Er, Yb, Lu) ceramics to replace YTaO$_4$ to obtain TBCs with lower thermal conductivity and better fracture toughness at high temperature. Previous studies [9,10] report that the rare-earth tantalates RETaO$_4$ have a relatively high RE^{3+} concentration, will be new promising candidate materials for microchip lasers and have attracted much attention as potential rare-earth-doped laser hosts. M. Nyman et al. [11] report that doped and undoped RETaO$_4$ have chemical stability and show many other promising characteristics such as photoelectronic activity, ion conductivity and luminescence. However, in our work, lanthanum rare-earth tantalates (RETaO$_4$) materials are proposed as the next-generation thermal barrier coatings because of their excellent thermal properties and low hardness at high temperature.

In this work, lanthanum rare-earth tantalates (RETaO$_4$) materials were investigated in terms of the synthesis, Vickers hardness, heat capacity, thermal diffusivities and conductivities. The low thermal conductivity is one of the critical requirements for TBCs. Lanthanum rare-earth tantalate (RETaO$_4$) ceramics can be used as TBCs when the temperature is expected to exceed 1600 °C.

The RETaO$_4$ ceramics were fabricated using a solid-state reaction. More information about the preparation process and measurement equipment is provided in the Supplementary materials.

The XRD patterns of the samples are shown in Fig. 1(a). From these patterns, the observed peaks are notably consistent with the JCPDS data card: 83-0408, 24-0412, 24-0441, 12-0379, 24-0407, 24-1415 and 24-1263 for NdTaO$_4$, EuTaO$_4$, GdTaO$_4$, DyTaO$_4$, ErTaO$_4$, YbTaO$_4$ and LuTaO$_4$, respectively, indicate that the RETaO$_4$ ceramics were successfully synthesized. The XRD analysis results demonstrate that NdTaO$_4$, EuTaO$_4$, DyTaO$_4$, GdTaO$_4$ and ErTaO$_4$ were in the m phase, and YbTaO$_4$ and LuTaO$_4$ were the m' phase. The XRD patterns show that the peaks at 15–70° were the monoclinic phase with no evidence of impurity. The space group, lattice parameters, cell volume, crystal density and porosity of RETaO$_4$ are listed in Table 1, which show that the lattice parameter (a, b, c) increased with the increase in radius of the RE^{3+} ion. A larger radius of the RE^{3+} ion causes an increase in crystalline volume and a decrease in bulk density, which contribute to reducing the thermal conductivity of RTaO$_4$ ceramics.

Fig. 1(b) shows that the vibrational modes of GdTaO$_4$, ErTaO$_4$, NdTaO$_4$, EuTaO$_4$ and DyTaO$_4$ of m phase with space group I2 (5) are

* Corresponding author.
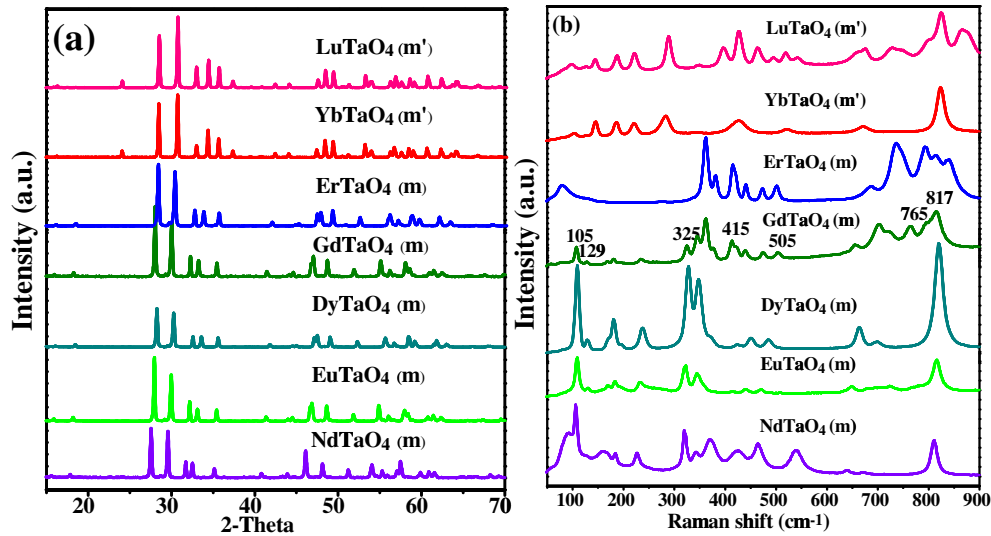 *E-mail address:* jingfeng@kmust.edu.cn (J. Feng).

Fig. 1. (a) XRD patterns and ICDD PDF data of RETaO$_4$ (RE = Nd, Eu, Gd, Dy, Er, Yb, Lu) ceramics; (b) room-temperature Raman spectrum of the samples.

similar. However, because of the different effects of RE^{3+} on different physical properties (e.g., atomic mass, RE^{3+} ionic radius and electronegativity of lanthanide ions), some Raman peaks exhibited different characters depending on RE^{3+}. NdTaO$_4$ and DyTaO$_4$ have a notably strong band near 105 cm^{-1}, but the energy of the Raman peaks of GdTaO$_4$, ErTaO$_4$, and EuTaO$_4$ was weak. Thus, the Raman peaks near 105 cm^{-1} are the antisymmetric stretching vibration of Ta—O bonds. For the Raman peaks in the ranges of 129–325 cm^{-1} and 505–765 cm^{-1}, which were notably weak because of the effects of molecular vibration (RETaO$_4$), the law curve of Raman bands of RETaO$_4$ was difficult to observe in this region. The Raman peaks at 325–415 cm^{-1} can be the vibration coupling interaction of RE-Ta-O. The bands at 817 ± 10 cm^{-1} were notably strong, which was an overtone bands associated with Ta—O bonds. The low-frequency bands are generally assigned to the bending vibration [12]; the Raman peaks at 415–505 cm^{-1} are the low frequencies associated with the bending vibration of RE—O bonds.

However, the Raman frequency of YbTaO$_4$ and LuTaO$_4$ of the m′ phase were not consistent with that of m-phase RETaO$_4$, which may be the effect of the chemical bonds and space groups. The Raman frequencies varied for different chemical bonds; for example, the Yb—O and Nd—O, Lu—Ta and Eu—Ta ionic bonding had different Raman frequencies. The YbTaO$_4$ and LuTaO$_4$ compounds were m′ phase with the space group P2/a (13); the others were m phase with the space group I2 (5). According to group theory, the difference in crystalline symmetry and vibration mode between m and m′ phases may cause the Raman shifts. Compared with the m phase, YbTaO$_4$ and LuTaO$_4$ in the m′ phase have larger mean atomic mass and shorter ion radius, which increase the crystalline volume and decrease the bulk density. Thus, the anharmonic vibration among the atoms is strong.

The typical microstructures of RETaO$_4$ samples are shown in Fig. 2. The grain boundary among the grains was obvious. Granular RETaO$_4$

was observed in the microstructure, and the grain size of the samples was approximately 2–14 μm. In addition, the pores were apparent in the ceramics, which can decrease the hardness, bending strength and creep resistance of the samples.

Based on Neumann–Kopp law [13], the specific heat capacity of the RETaO$_4$ specimens was calculated as a sum of the atomic heat capacities of the constituent oxides. The specific heat of the compounds is shown in Fig. 3(a). The specific heat capacity rapidly increased with increasing temperature because of the volumetric expansion and phonon excitation. The RETaO$_4$ specimens had a much lower heat capacity than 7-8YSZ [14,15], which decreased the thermal conductivity of RETaO$_4$ ceramics.

The thermal diffusivities of the RETaO$_4$ samples are shown in Fig. 3(b). The RETaO$_4$ specimens with a higher thermal diffusivity at low temperatures slowly decreased with increasing temperature possibly because of the effect of the porosity and phonon conduction behavior. Fig. 2 shows that the sintered specimens still contained pores; the higher porosity would lead to stronger phonon scattering, which could decrease the thermal diffusivity. RETaO$_4$ had higher thermal diffusivities than 7YSZ [14] at low temperatures. The reason can be that 7YSZ has many oxygen vacancies at low temperatures, which weakly affect the thermal diffusivities. The anharmonic effect was obvious when the temperature increased, so 7YSZ has higher thermal diffusivities than RETaO$_4$ ceramics at high temperatures.

The thermal conductivities of the RETaO$_4$ (RE = Nd, Eu, Gd, Dy, Er, Yb, Lu) ceramics are plotted versus temperature in Fig. 4(c). When the temperature increased from 100 °C to 800 °C, the conductivity variation trends gradually decreased, which may be explained as follows. At low temperatures, the mean free path of phonons is determined by factors such as the inter-defect distance, grain size or grain boundary. The phonon mean free path l can be divided into several independent parts as

Table 1
The space group, lattice parameters, cell volume, crystal density and porosity of RETaO$_4$ ceramics.

Samples	Space group	a (Å)	b (Å)	c (Å)	Radius (nm)	Cell volume (Å^3)	Theoretical density (g/cm^3)	Experimental density (g/cm^3)	Porosity (%)
NdTaO$_4$	I2 (5)	5.5205	11.2581	5.1203	0.0983	316.65	8.164	7.519	8
EuTaO$_4$	I2 (5)	5.4127	11.0740	5.0848	0.0938	303.33	8.807	8.252	6
GdTaO$_4$	I2 (5)	5.4339	11.1122	5.0862	0.0947	305.61	8.626	8.276	4
DyTaO$_4$	I2 (5)	5.3556	10.9805	5.06174	0.0912	296.26	9.080	8.389	8
ErTaO$_4$	I2 (5)	5.3169	10.9103	5.0503	0.089	291.61	9.389	8.480	9
YbTaO$_4$	P2/a (13)	5.2528	5.4298	5.0702	0.0868	143.77	9.655	8.704	9
LuTaO$_4$	P2/a (13)	5.2382	5.4298	5.0604	0.0861	143.13	9.620	8.875	8